Far-Field Superresolution of Thermal Electromagnetic Sources at the Quantum Limit

Ranjith Nair[1,*] and Mankei Tsang[1,2]
[1]Department of Electrical and Computer Engineering, National University of Singapore, 4 Engineering Drive 3, 117583 Singapore
[2]Department of Physics, National University of Singapore, 2 Science Drive 3, 117551 Singapore
(Received 6 July 2016; published 4 November 2016)

We obtain the ultimate quantum limit for estimating the transverse separation of two thermal point sources using a given imaging system with limited spatial bandwidth. We show via the quantum Cramér-Rao bound that, contrary to the Rayleigh limit in conventional direct imaging, quantum mechanics does not mandate any loss of precision in estimating even deep sub-Rayleigh separations. We propose two coherent measurement techniques, easily implementable using current linear-optics technology, that approach the quantum limit over an arbitrarily large range of separations. Our bound is valid for arbitrary source strengths, all regions of the electromagnetic spectrum, and for any imaging system with an inversion-symmetric point-spread function. The measurement schemes can be applied to microscopy, optical sensing, and astrometry at all wavelengths.

DOI: 10.1103/PhysRevLett.117.190801

The Rayleigh criterion for resolving two incoherent optical point sources [1] is the most widely used benchmark for the resolving power of an imaging system. According to it, the sources can be resolved by direct imaging only if they are separated by at least the diffraction-limited spot size of the point-spread function of the imaging system. While the criterion is heuristic and does not take into account the intensity of the sources or the measurement shot noise, recent work [2–5] has made it rigorous by taking as resolution measure the classical Cramér-Rao lower bound (CRB) of estimation theory [6] on the mean-squared error (MSE) of any unbiased estimate of the separation of the sources using spatially resolved image-plane photon counting. These works showed that if the detected average photon number per mode $N_s \ll 1$, the MSE of any unbiased estimator based on direct imaging diverges as the source separation decreases to 0 over an interval comparable to the Rayleigh limit. This phenomenon, dubbed Rayleigh's curse in Ref. [7], stems from the indistinguishability between the photons coming from the two sources and imposes a fundamental limitation of direct imaging in resolving sources much closer than the spot size, even when the measured photon number is taken into account. Recent developments in far-field microscopy [8] sidestep Rayleigh's curse by preventing multiple sources from emitting simultaneously, but control over the emission properties of sources is unavailable in target sensing or astronomical imaging.

While the development of novel quantum states of light and measurement techniques has given rise to the vast field of quantum imaging [9], fundamental quantum limits in resolving two incoherent sources have been largely neglected since the early days of quantum estimation theory [10,11]. Recently, the coherent [12] and incoherent [7] two-source resolution problems were revisited using the quantum Cramér-Rao bound (QCRB) [11,13] that accounts for all (unbiased) measurement techniques allowed by quantum mechanics. Under a weak-source assumption similar to that in Refs. [2–5], it was found in Ref. [7] that the QCRB, unlike the CRB for direct imaging, showed no dependence on the separation of the sources. Linear-optics-based measurements that approach the bound were also proposed [7,14]. Subsequent demonstrations of superresolution [15–18] have substantiated the feasibility of these proposals. Nevertheless, the classical treatments [2–5] and the quantum treatment [7] neglect multiphoton coincidences and bunching, phenomena that figure prominently in quantum optics [19]. While such an approximation leads to correct conclusions for weak sources, e.g., at optical frequencies [20], it is problematic for intense sources, e.g., in the microwave to far-infrared regimes, for high-temperature astronomical sources, and for optical demonstrations using pseudothermal light generated from laser sources [21]. As such, a quantum-optically rigorous derivation of the resolution limit is as yet unavailable.

In this Letter, we solve these problems and obtain the QCRB for estimating the separation of two thermal point sources of arbitrary strength using rigorous quantum optics and estimation theory and show that resolution is not fundamentally compromised at sub-Rayleigh separations. We then propose two schemes that approach the QCRB. The finite spatial-mode demultiplexing (fin-SPADE) scheme performs photon counting in a finite number of suitably chosen transverse spatial modes of the field. The interferometric pixelated superlocalization by image inversion interferometry (pix-SLIVER) scheme uses pixelated detector arrays in the two interferometer outputs. The two schemes approach the QCRB over greater ranges of the separation as the number of accessed modes (fin-SPADE) or the number of pixels (pix-SLIVER) is increased.

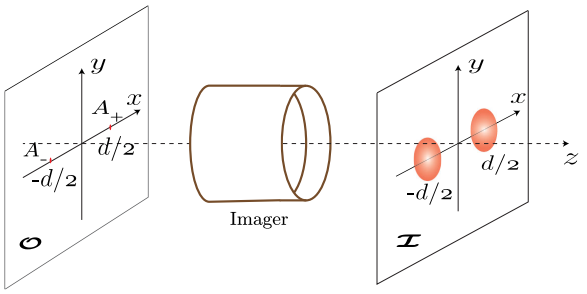

FIG. 1. A spatially invariant imaging system. Point sources at $(\pm d/2, 0)$ of the object plane O have images centered at $(\pm d/2, 0)$ of the image plane I but spread out by the PSF of the system.

Source and system model.—Consider two thermal point sources being imaged under paraxial conditions by a spatially invariant unit-magnification imaging system (Fig. 1)—such an assumption entails no essential loss of generality [22]. We assume that the system's amplitude point-spread function (PSF) $\psi(\boldsymbol{\rho})[\int_I d\boldsymbol{\rho}|\psi(\boldsymbol{\rho})|^2 = 1]$ is inversion symmetric, i.e., $\psi(-\boldsymbol{\rho}) = \psi(\boldsymbol{\rho})$, where $\boldsymbol{\rho} = (x, y)$ is the transverse coordinate in the image plane I. Most imaging systems, e.g., those with circular or rectangular entrance pupils, satisfy this assumption [22].

Two incoherent thermal point sources, each of effective strength (average photon number) N_s [23], are described by a pair of dimensionless amplitudes $A = (A_+, A_-) \in \mathbb{C}^2$ with the joint probability density [19,24]:

$$P_{N_s}(A) = (\pi N_s)^{-2} \exp\left[-(|A_+|^2 + |A_-|^2)/N_s\right]. \quad (1)$$

In order to focus on the essential physics of the problem, we assume that the centroid (midpoint) of the sources is imaged at the optical axis and that the line joining the sources is aligned with the x axis, so that images of the sources are centered at $\boldsymbol{d}_\pm = (\pm d/2, 0)$, respectively, in the image plane. Estimating the centroid of two incoherent sources by direct imaging is subject to much less stringent bounds than the separation [2,7,11] and may be done using a portion of the available signal [7]. We also assume that only a single quasimonochromatic temporal mode $\xi(t)[\int_0^T dt|\xi(t)|^2 = 1]$ is excited over the observation interval $[0, T]$. Extensions to multiple temporal modes can be made using standard techniques [11].

Conditioned on the value of A, the electromagnetic field in the image plane, described by the positive-frequency field operator $\hat{E}(\boldsymbol{\rho}, t)$ [25], is in a pure coherent state $|\psi_{A,d}\rangle$ that is an eigenstate of $\hat{E}(\boldsymbol{\rho}, t)$ with the eigenfunction $\psi_{A,d}(\boldsymbol{\rho}, t)$ given by

$$\hat{E}(\boldsymbol{\rho}, t)|\psi_{A,d}\rangle = \psi_{A,d}(\boldsymbol{\rho}, t)|\psi_{A,d}\rangle, \quad (2)$$

$$\psi_{A,d}(\boldsymbol{\rho}, t) = [A_+\psi(\boldsymbol{\rho} - \boldsymbol{d}_+) + A_-\psi(\boldsymbol{\rho} - \boldsymbol{d}_-)]\xi(t), \quad (3)$$

where we have used linearity and the spatial invariance of the imaging system to write (3). The unconditional quantum state ρ_d then has the P representation [19]

$$\rho_d = \int_{\mathbb{C}^2} d^2A_+ d^2A_- P_{N_s}(A)|\psi_{A,d}\rangle\langle\psi_{A,d}|. \quad (4)$$

Fundamental quantum bound.—The quantum Fisher information (QFI) $\mathcal{K}_d$ of the state family $\{\rho_d\}$ determines the QCRB

$$\mathbb{E}[\check{d} - d]^2 \geq \mathcal{K}_d^{-1} \quad (5)$$

on the MSE of an unbiased estimator $\check{d}$ of the separation derived from *any* quantum measurement [11,13,26]. Our derivation of $\mathcal{K}_d$ proceeds by calculating the quantum fidelity $F(\rho_{d_1}, \rho_{d_2}) = \mathrm{Tr}\sqrt{\sqrt{\rho_{d_1}}\rho_{d_2}\sqrt{\rho_{d_1}}}$ between the (noncommuting) states (4) for two neighboring separations d_1 and d_2 and employing the relation

$$\mathcal{K}_d = 8 \times \lim_{d_1, d_2 \to d} \frac{1 - F(\rho_{d_1}, \rho_{d_2})}{(d_1 - d_2)^2} \quad (6)$$

between the fidelity and the QFI [26,27]. The details of the derivation are given in Ref. [28], with the result

$$\mathcal{K}_d = -2\beta(0)N_s - 2\gamma^2(d)\left[\frac{(1 + N_s)N_s^2}{(1 + N_s)^2 - \delta^2(d)N_s^2}\right], \quad (7)$$

where

$$\delta(d) = \int_I d\boldsymbol{\rho}\psi^*(\boldsymbol{\rho})\psi(\boldsymbol{\rho} - (d, 0)) \quad (8)$$

is the overlap function of the PSF for translations in the x direction, $\gamma(d) = \partial\delta(d)/\partial d$, and $\beta(d) = \partial\gamma(d)/\partial d$ [30]. In particular,

$$-\beta(0) = \int_I d\boldsymbol{\rho}\left|\frac{\partial\psi(\boldsymbol{\rho})}{\partial x}\right|^2 \equiv (\Delta k_x^2), \quad (9)$$

the mean-squared spatial bandwidth of the PSF in the x direction, and is independent of orientation for circular-symmetric PSFs. The first term in (7)—identical to the result in Ref. [7]—is independent of d and dominates in the $N_s \ll 1$ regime. For arbitrary N_s, this value is attained in the large-d limit [$\gamma(d) \to 0$ as $d \to \infty$] but also for $d = 0$, so that Rayleigh's curse is evaded. The QFI suffers a dip at intermediate values whose relative depth increases with increasing N_s. This is the net effect of correcting the overestimation of the single-photon probability and neglect of multiphoton events in the weak-source model of Ref. [7]. The QFI (7) and a lower bound on the FI of spatially resolved direct detection (see the following) are shown in Fig. 2 for a system with the circular Gaussian PSF

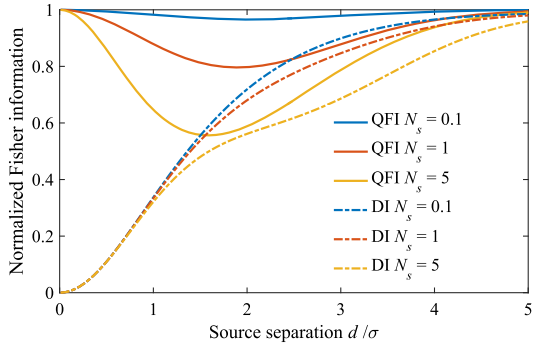

FIG. 2. The QFI of Eq. (7) (solid lines) and the lower bound of Eq. (12) (dash-dotted lines) on spatially and number-resolved direct imaging (DI) for the Gaussian PSF (10). The plots are normalized to the respective maximum values $N_s/2\sigma^2$ of the QFI and are independent of the PSF half-width σ.

$$\psi_G(\boldsymbol{\rho}) = (2\pi\sigma^2)^{-1/2} \exp\left[-|\boldsymbol{\rho}|^2/(4\sigma^2)\right], \tag{10}$$

for which $-\beta(0) = 1/(4\sigma^2)$.

The QFI can in principle be attained using multistep measurements [31,32], but we now give two linear-optics schemes that closely approach it.

Fin-SPADE.—For a system with the Gaussian PSF (10), consider the separation of the image-plane field $\hat{E}(\boldsymbol{\rho}, t)$ into its components in the transverse electromagnetic (TEM_{q0}) Hermite-Gaussian (HG) basis [33] $\{\psi_{q0}(\boldsymbol{\rho})\}_q$ with $\psi_G(\boldsymbol{\rho}) \equiv \psi_{00}(\boldsymbol{\rho})$, followed by number-resolved but not necessarily time-resolved photon counting over $[0, T]$ in each of the modes with order $0 \le q \le Q$. The coupling to the TEM_{q0} modes can be accomplished (Fig. 3) in the same way as SPADE [7]. Mathematically, fin-SPADE implements a simultaneous measurement of the operators $\{\hat{N}_q = \hat{a}_q^\dagger \hat{a}_q\}_{q=0}^{Q}$ with

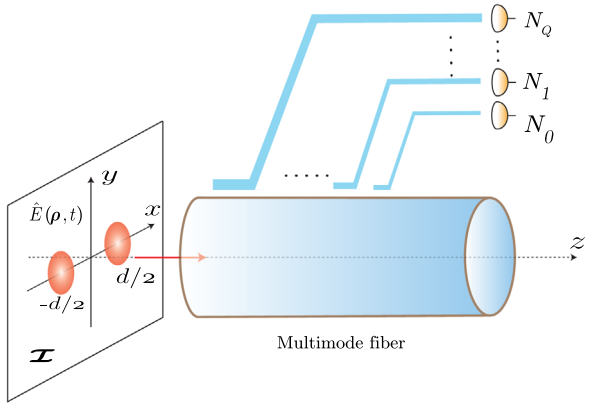

FIG. 3. Fin-SPADE. The image-plane field is coupled into a multimode fiber and separated into its components in the Hermite-Gaussian TEM_{q0} modes of order $0 \le q \le Q$ by evanescent coupling to single-mode fibers supporting those modes. Detectors record the photon number in each mode.

$$\hat{a}_q = \int_0^T dt \int_I d\boldsymbol{\rho} \hat{E}(\boldsymbol{\rho}, t) \psi_{q0}^*(\boldsymbol{\rho}) \xi^*(t), \tag{11}$$

resulting in a $(Q+1)$ vector $\boldsymbol{N} = (N_0, \ldots, N_Q)^\mathsf{T}$ of the number of counts in each mode.

The statistical correlations among the HG modes in the state (4) make calculation of the FI $\mathcal{J}_d[\boldsymbol{N}]$ of fin-SPADE difficult. We turn instead to a general lower bound on the FI $\mathcal{J}_x[\boldsymbol{Y}]$ on an arbitrary parameter x of any vector observation $\boldsymbol{Y} = (Y_1, \ldots, Y_M)^\mathsf{T} \in \mathbb{R}^M$ depending on x. For $\boldsymbol{\mu} = (\langle Y_1 \rangle_x, \ldots, \langle Y_M \rangle_x)^\mathsf{T}$ the mean vector and $\boldsymbol{C} = \langle (\boldsymbol{Y} - \boldsymbol{\mu})(\boldsymbol{Y} - \boldsymbol{\mu})^\mathsf{T} \rangle_x$ the covariance matrix of $\boldsymbol{Y}$ evaluated at x, we have [34]

$$\mathcal{J}_x[\boldsymbol{Y}] \ge \dot{\boldsymbol{\mu}}^\mathsf{T} \boldsymbol{C}^{-1} \dot{\boldsymbol{\mu}}, \tag{12}$$

where $\dot{\boldsymbol{\mu}} = \partial \boldsymbol{\mu}/\partial x$. Formally similar expressions have appeared in the quantum estimation literature [35].

The mean and covariance of $\boldsymbol{N}$ in the state ρ_d for the fin-SPADE measurement can be calculated using semiclassical photodetection theory [36] as detailed in Ref. [28]. The resulting bound (12) is plotted in Fig. 4 for a representative value of $N_s = 1.5$ photons. Also shown is the lower bound (12) on the FI of spatially resolved direct imaging (see also Figs. 2 and 6 and Ref. [28] for details). Direct imaging is near-quantum optimal for $d \gtrsim 2\sigma$—in this regime, interference between the sources is minimal and the QCRB follows that for localizing a single source [7,11]. We see that measuring the first six HG modes already achieves the quantum bound (7) over the range $d = 0$–4σ and that

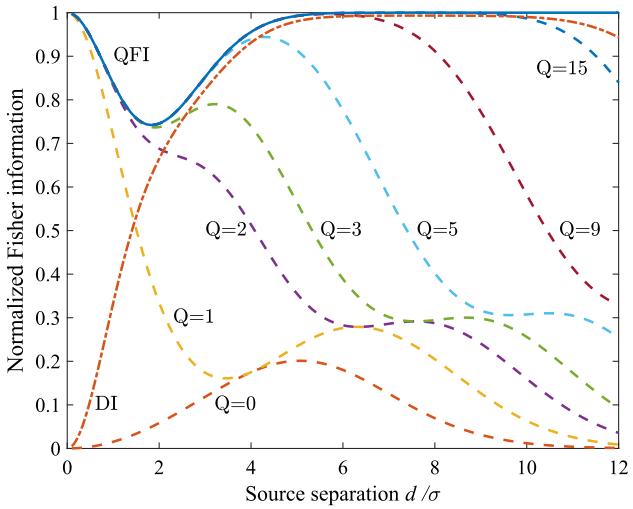

FIG. 4. Fin-SPADE performance. The QFI (solid line), the lower bound (12) on the FI of fin-SPADE (dashed lines) for various Q, and of DI (dash-dotted line). The Gaussian PSF (10) is assumed, and $N_s = 1.5$ photons. The plots are normalized to the maximum value $N_s/2\sigma^2$ of the QFI and are independent of σ. The DI bound assumes a detector of width 17σ with $P_d = 50$ pixels at 100% fill factor and is stable to increase in P_d. Number-resolving unity-quantum-efficiency detectors are assumed for all the measurement schemes.

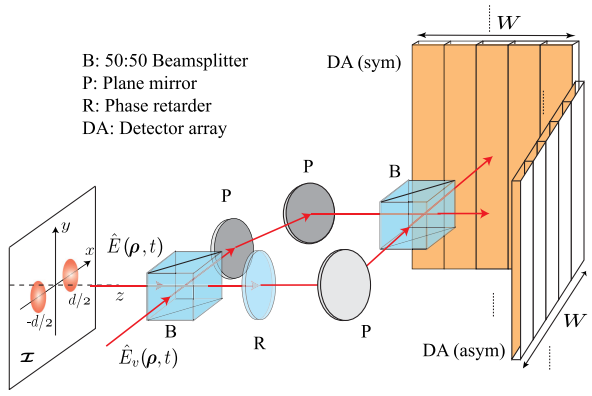

FIG. 5. Pix-SLIVER. The image-plane field is separated into its symmetric and antisymmetric components (13) using a balanced Mach-Zehnder interferometer with an extra reflection in one arm before detecting the two outputs using identical detector arrays of width W pixelated in the x direction.

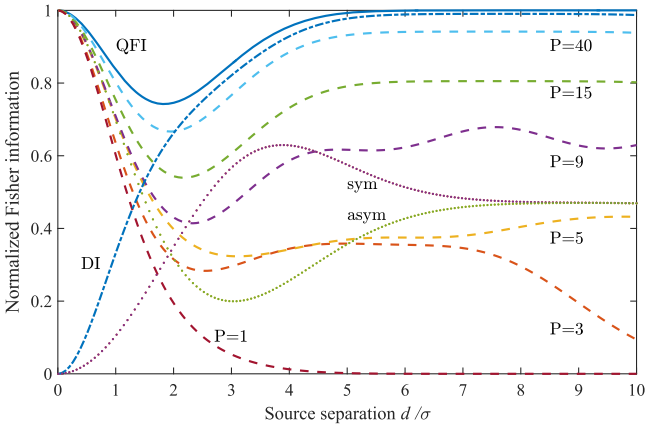

FIG. 6. Pix-SLIVER performance. The QFI (solid line), the lower bound (12) on the FI of pix-SLIVER using on-off detection with various P values (dashed lines), the lower bound (12) for DI (dash-dotted line) with number-resolved detection, and the contributions of the symmetric (sym) and antisymmetric (asym) field components to (12) for $P = 40$ (dotted lines). The Gaussian PSF (10) is assumed, and $N_s = 1.5$ photons. The plots are normalized to the maximum value $N_s/2\sigma^2$ of the QFI and are independent of σ. The lower bounds assume detector array(s) of width 17σ and 100% fill factor. The DI bound assumes an array with $P_d = 50$ pixels and is stable to increase in P_d.

increasing Q widens the region of saturation of the quantum bound.

Pix-SLIVER.—Consider a PSF that is reflection symmetric about the y axis, i.e., $\psi(-x,y) = \psi(x,y)$, but otherwise arbitrary. Figure 5 shows a schematic of pix-SLIVER. Using an extra reflection in one arm of a balanced Mach-Zehnder interferometer, we separate the image-plane field into its symmetric (s) and antisymmetric (a) components with respect to inversion of the image-plane field operator in the x axis. The output field operators are

$$\hat{E}^{s\text{ or }a}(x,y,t) = [\hat{E}(x,y,t) \pm \hat{E}(-x,y,t)]/2 + [\hat{E}_v(x,y,t) \mp \hat{E}_v(-x,y,t)]/2, \quad (13)$$

where $\hat{E}_v(\boldsymbol{\rho},t)$ is the (vacuum-state) field operator entering the empty port of the first beam splitter in Fig. 5. The two outputs are detected using two detector arrays pixelated along the x direction. Each array consists of P pixels of equal x width. To show that superresolution is possible without number-resolving detectors, we assume *on-off* detection in each pixel. For a pixel $p \in \{1,\ldots,P\}$ in the $\alpha \in \{s,a\}$ array, such a measurement corresponds to measuring the operator $\hat{K}_p^{(\alpha)} = f(\hat{N}_p^{(\alpha)})$, where

$$\hat{N}_p^{(\alpha)} = \int_0^T dt \int_{A_p^{(\alpha)}} d\boldsymbol{\rho}\hat{E}^{(\alpha)\dagger}(\boldsymbol{\rho},t)\hat{E}^{(\alpha)}(\boldsymbol{\rho},t) \quad (14)$$

is the total photon number operator measured over the pixel area $A_p^{(\alpha)}$ of array α, and $f(x) = 0$ if $x = 0$ and 1 otherwise. The mean and covariance of the observation $\boldsymbol{K} = (K_1^{(s)},\ldots,K_P^{(s)},K_1^{(a)},\ldots,K_P^{(a)})$ are calculated in Ref. [28]. For the Gaussian PSF (10), the lower bound on the FI $\mathcal{J}_d[\boldsymbol{K}]$ of pix-SLIVER is plotted in Fig. 6 for various values of P, showing how the QFI can be approached more and more closely over the entire range of separation values by increasing P.

Discussion.—The sensitivity of our schemes at sub-Rayleigh separations can be intuitively understood as follows. Information on d is encoded in the energy distribution in any basis of spatial modes on I, each of which is in a thermal state. The FI of any one mode scales roughly as $\sim[\bar{N}'(d)/\bar{N}(d)]^2$ [14], for $\bar{N}(d)$ the mean energy in the mode and $\bar{N}'(d) = \partial\bar{N}(d)/\partial d$, and is large if $\bar{N}(d) \sim 0$. For fin-SPADE, while most of the energy is concentrated in the TEM_{00} mode, most of the FI is contributed by the TEM_{10} mode (Fig. 4). Direct imaging is a poor way to estimate the energy in the latter, since the much larger energy in the TEM_{00} mode acts like background noise. Similarly, in pix-SLIVER, the antisymmetric component (comprising the odd modes in any basis of modes with definite parity about the centroid) carries the most information at sub-Rayleigh separations (Fig. 6).

While the QCRB can be approached by the maximum-likelihood estimator in the limit of a large number of measurements [6], suboptimal estimators can also evade Rayleigh's curse [15–18]. That small values of P achieve a substantial fraction of the QFI in pix-SLIVER is in line with work on detecting beam displacements using pixelated detectors [37]. The optical components used in pix-SLIVER have counterparts in other regions of the electromagnetic spectrum, leading to potential applications from the microwave to the γ-ray regions [38]. Generalizations to 2D separation estimation [39] and variants of pix-SLIVER using image inversion devices [40] can be envisaged.

Recently developed techniques [41] may help to generalize our quantum limit to multiple parameters and to unequal source strengths.

This work is supported by the Singapore National Research Foundation under NRF Grant No. NRF-NRFF2011-07 and the Singapore Ministry of Education Academic Research Fund Tier 1 Project No. R-263-000-C06-112. R. N. developed the source model, obtained the QFI, and invented pix-SLIVER. M. T. and R. N. bounded the FI of fin-SPADE, and R. N. applied (12) to all the detection schemes.

Note added.—Recently, we became aware of an alternative derivation by Lupo and Pirandola [42] of a more general quantum bound applicable to arbitrary quantum states, including our bound Eq. (7) for thermal sources as a special case. Our proposal of concrete measurement schemes and their near-optimality for a broad range of source separations, however, are unique results here.

*Corresponding author.
elernair@nus.edu.sg

[1] L. Rayleigh, Philos. Mag. J. Sci. **8**, 261 (1879); M. Born and E. Wolf, *Principles of Optics: Electromagnetic Theory of Propagation, Interference and Diffraction of Light* (Cambridge University Press, Cambridge, 1999).
[2] E. Bettens, D. Van Dyck, A. Den Dekker, J. Sijbers, and A. Van den Bos, Ultramicroscopy **77**, 37 (1999).
[3] S. V. Aert, A. den Dekker, D. V. Dyck, and A. van den Bos, J. Struct. Biol. **138**, 21 (2002).
[4] S. Ram, E. S. Ward, and R. J. Ober, Proc. Natl. Acad. Sci. U.S.A. **103**, 4457 (2006).
[5] J. Chao, E. S. Ward, and R. J. Ober, J. Opt. Soc. Am. A **33**, B36 (2016).
[6] H. Cramér, *Mathematical Methods of Statistics (PMS-9)*, Vol. 9 (Princeton University Press, Princeton, 2016); C. R. Rao, Bull. Calcutta Math. Soc. **37**, 81 (1945); H. L. Van Trees, *Detection, Estimation, and Modulation Theory: Part I*, 1st ed. (Wiley-Interscience, New York, 2001).
[7] M. Tsang, R. Nair, and X.-M. Lu, Phys. Rev. X **6**, 031033 (2016).
[8] S. Weisenburger and V. Sandoghdar, Contemp. Phys. **56**, 123 (2015).
[9] L. A. Lugiato, A. Gatti, and E. Brambilla, J. Opt. B **4**, S176 (2002); Y. Shih, IEEE J. Sel. Top. Quantum Electron. **13**, 1016 (2007); *Quantum Imaging*, edited by M. I. Kolobov (Springer Science & Business Media, New York, 2007).
[10] C. W. Helstrom, IEEE Trans. Inf. Theory **19**, 389 (1973).
[11] C. W. Helstrom, *Quantum Detection and Estimation Theory* (Academic, New York, 1976).
[12] M. Tsang, Optica **2**, 646 (2015).
[13] A. S. Holevo, *Probabilistic and Statistical Aspects of Quantum Theory* (Edizioni della Normale, Pisa, 2011).
[14] R. Nair and M. Tsang, Opt. Express **24**, 3684 (2016).
[15] Z. S. Tang, K. Durak, and A. Ling, Opt. Express **24**, 22004 (2016).
[16] F. Yang, A. Taschilina, E. S. Moiseev, C. Simon, and A. I. Lvovsky, Optica **3**, 1148 (2016).
[17] W. K. Tham, H. Ferretti, and A. M. Steinberg, arXiv:1606.02666.
[18] M. Paúr, B. Stoklasa, Z. Hradil, L. L. Sánchez-Soto, and J. Rehacek, Optica **3**, 1144 (2016).
[19] L. Mandel and E. Wolf, *Optical Coherence and Quantum Optics* (Cambridge University Press, Cambridge, 1995).
[20] J. Zmuidzinas, J. Opt. Soc. Am. A **20**, 218 (2003); M. Tsang, Phys. Rev. Lett. **107**, 270402 (2011).
[21] L. E. Estes, L. M. Narducci, and R. A. Tuft, J. Opt. Soc. Am. **61**, 1301 (1971).
[22] J. W. Goodman, *Introduction to Fourier Optics*, 3rd ed. (Roberts, Englewood, 2005).
[23] To be precise, N_s is the average number of photons from each source reaching the image plane, allowing us to write Eqs. (2) and (3).
[24] J. W. Goodman, *Statistical Optics* (Wiley, New York, 1985).
[25] We assume a single polarization and that the quasimonochromatic scalar field operator $\hat{E}(\boldsymbol{\rho}, t)$ has been cast in units of $\sqrt{\text{photons m}^{-2}\,\text{s}^{-1}}$.
[26] M. Hayashi, *Quantum Information* (Springer, New York, 2006).
[27] S. L. Braunstein and C. M. Caves, Phys. Rev. Lett. **72**, 3439 (1994).
[28] See Supplemental Material at http://link.aps.org/supplemental/10.1103/PhysRevLett.117.190801 for supporting calculations, which also cites Ref. [29].
[29] C. Gerry and P. Knight, *Introductory Quantum Optics* (Cambridge University Press, Cambridge, 2005).
[30] Inversion symmetry of the PSF entails that $\delta(d) = \delta(-d) = \delta^*(d)$ [28]. Note that $\delta(d) \leq \delta(0) = 1$, so that $\gamma(0) = 0$.
[31] *Asymptotic Theory of Quantum Statistical Inference: Selected Papers*, edited by M. Hayashi (World Scientific, Singapore, 2005).
[32] A. Fujiwara, J. Phys. A **39**, 12489 (2006).
[33] A. Yariv, *Quantum Electronics* (Wiley, New York, 1989).
[34] M. Stein, A. Mezghani, and J. A. Nossek, IEEE Signal Process. Lett. **21**, 796 (2014).
[35] M. Hotta and M. Ozawa, Phys. Rev. A **70**, 022327 (2004); W. Zhong, X.-M. Lu, X. X. Jing, and X. Wang, J. Phys. A **47**, 385304 (2014).
[36] J. H. Shapiro, IEEE J. Sel. Top. Quantum Electron. **15**, 1547 (2009).
[37] G. C. Knee and E. M. Gauger, Phys. Rev. X **4**, 011032 (2014).
[38] R. Adam *et al.*, arXiv:1502.01582; K. C. Patel and S. R. Spath, Proc. SPIE Int. Soc. Opt. Eng. **5487**, 112 (2004); M. C. Weisskopf, The Chandra X-Ray Observatory, NASA Technical Report No. MSFC-E-DAA-TN27074, 2015; T. C. Weekes, *Very High Energy Gamma-Ray Astronomy* (CRC Press, Boca Raton, 2003).
[39] S. Z. Ang, R. Nair, and M. Tsang, arXiv:1606.00603.
[40] K. Wicker and R. Heintzmann, Opt. Express **15**, 12206 (2007); K. Wicker, S. Sindbert, and R. Heintzmann, Opt. Express **17**, 15491 (2009).
[41] P. Marian and T. A. Marian, Phys. Rev. A **86**, 022340 (2012); L. Banchi, S. L. Braunstein, and S. Pirandola, Phys. Rev. Lett. **115**, 260501 (2015).
[42] C. Lupo and S. Pirandola, following Letter, Phys. Rev. Lett. **117**, 190802 (2016).